Similarity Measures for Closed General Type-2 Fuzzy Sets: Overview, Comparisons, and a Geometric Approach

Dongrui Wu, *Senior Member, IEEE*, and Jerry M. Mendel, *Life Fellow, IEEE*

***Abstract*—The similarity between two fuzzy sets (FSs) is an important concept in fuzzy logic. As the research interest on general type-2 (GT2) FSs has increased recently, many similarity measures for them have also been proposed. This paper gives a comprehensive overview of existing similarity measures for GT2 FSs, points out their limitations, and, by using an intuitive geometric explanation, proposes a Jaccard similarity measure for GT2 FSs that is an extension of the popular Jaccard similarity measure for type-1 and interval type-2 FSs. The fundamental difference between the proposed Jaccard similarity measure for GT2 FSs and all existing similarity measures is that the Jaccard similarity measure considers the overall geometries of two GT2 FSs and does not depend on a specific representation of the GT2 FSs, whereas all existing similarity measures for GT2 FSs depend either on the vertical slice representation or the α-plane representation. We show that the Jaccard similarity measure for GT2 FSs satisfies four properties of a similarity measure and demonstrate its reasonableness using two examples.**

***Index Terms*—General type-2 fuzzy sets (GT2 FSs), interval type-2 fuzzy sets (IT2 FSs), similarity measure, type-1 fuzzy sets (T1 FSs).**

I. Introduction

TYPE-1 fuzzy set (T1 FS) theory was first proposed by Zadeh [39] in 1965 and has been successfully used in many applications. However, despite having a name that carries the connotation of uncertainty, research has shown that there are limitations in the ability of T1 FSs to model and minimize the effect of uncertainties [10], [11], [20], [36]. This is because a T1 FS is certain in the sense that its membership grades are crisp values. General type-2 (GT2) fuzzy sets (FSs) [40], characterized by membership grades that are themselves fuzzy, have been proposed to remedy this problem. GT2 FSs, and their simplified version, interval type-2 (IT2) FSs, have been shown to outperform T1 FSs in numerous applications [5], [11], [20], [36], [37].

Manuscript received August 31, 2017; revised May 5, 2018; accepted July 27, 2018. Date of publication August 2, 2018; date of current version February 27, 2019. *(Corresponding author: Dongrui Wu.)*

D. Wu is with the Key Laboratory of the Ministry of Education for Image Processing and Intelligent Control, School of Automation, Huazhong University of Science and Technology, Wuhan 430074, China (e-mail: drwu@hust.edu.cn).

J. M. Mendel is with the University of Southern California, Los Angeles, CA 90089 USA, and also with the College of Artificial Intelligence, Tianjin Normal University, Tianjin 300384, China (e-mail: mendel@sipi.usc.edu).

Color versions of one or more of the figures in this paper are available online at http://ieeexplore.ieee.org.

Digital Object Identifier 10.1109/TFUZZ.2018.2862869

The similarity between two FSs is a very important concept, with lots of applications. For example, Turksen and Zhong [27] proposed an approximate analogical reasoning schema, which uses an FS similarity measure to determine whether a rule should be fired, and a modification function inferred from a similarity measure to deduce a consequent. Setnes *et al.* [26] used the similarity measure of FSs for fuzzy rule-base simplification, where similar FSs were merged into a single common FS to replace them in the rule base. Candan *et al.* [4] proposed a similarity-based ranking and query-processing approach for multimedia databases. Mitchell [24] introduced a similarity measure for GT2 FSs, which was used for formulating classification problems in pattern recognition. Wu and Mendel [32] proposed a vector similarity measure for linguistic approximation, which maps the output of a computing-with-words engine into a word recommendation (linguistic label). They [33] also proposed a Jaccard similarity measure for IT2 FSs, which is more reliable and faster than the vector similarity measure and, hence, is more suitable for computing with words. Additionally, Wu and Mendel [34] proposed a similarity-based perceptual reasoning approach, which is an approximate reasoning method that can be used as a computing-with-words engine in perceptual computing [23]. Wagner *et al.* [29] proposed a nonsingleton fuzzy logic system, which computes the firing strength of each rule by the Jaccard similarity between the input and the antecedent FSs. It was applied to Mackey-Glass time-series predictions [29] and unmanned aerial vehicle control [8]. Bustince *et al.* [2] constructed similarity measures of T1 FSs based on restricted equivalence functions [1] and applied them to image thresholding. Galar *et al.* [9] further constructed an interval-valued (IV) similarity measure for IV FSs, based also on restricted equivalence functions, and applied it to stereo matching of color images.

Similarity measures for T1 and IT2 FSs have been extensively studied in the literature [7], [33]. Similarity measures for GT2 FSs[1] have also received considerable attention, and there have been many approaches [12]–[14], [18], [19], [24], [38], [42]. This paper gives a comprehensive overview of them.

The next section will show that a GT2 FS can be represented equivalently by several different representations. Because the similarity between two GT2 FSs is an intrinsic property that should not depend on a particular representation, theoretically it

[1]These GT2 FSs are called "closed" GT2 FSs, as explained in Section II-B.

should also be computed equivalently using different representations. Unfortunately, none of the existing similarity measures for GT2 FSs can satisfy this requirement. So, in this paper, we propose a geometry-based similarity measure for GT2 FSs, motivated from the popular Jaccard similarity measure for T1 and IT2 FSs, one that can be computed equivalently using different representations. Theoretical and experimental results verify its reasonableness.

The remainder of this paper is organized as follows. Section II briefly introduces some background knowledge on IT2 and GT2 FSs. Section III reviews existing similarity measures for GT2 FSs. Section IV proposes the Jaccard similarity measure for GT2 FSs. Section V compares these similarity measures using two examples. Finally, Section VI draws conclusions and points out some future research directions.

II. Background on IT2 and GT2 FSs

This section introduces the basic concepts of IT2 and GT2 FSs, which will be used in defining their similarity measures.

A. IT2 FSs

An IT2 FS [20] $\tilde{A}$ can be represented as

$$\tilde{A} = \{((x,u), \mu_{\tilde{A}}(x,u))\,|x \in X, u \in [0,1]\} \tag{1}$$

or, in FS notation, as

$$\tilde{A} = \bigcup_{x\in X} \bigcup_{u\in[0,1]} \mu_{\tilde{A}}(x,u)/(x,u). \tag{2}$$

In (1) and (2), x is called the *primary variable* and has domain X, $u \in [0,1]$ is called the *primary membership* or *secondary variable*, and $\mu_{\tilde{A}}(x,u)$ is called a *T2 membership function* (MF) or *secondary grade* for $\tilde{A}$, and it always equals 1 for an IT2 FS. At each value of x, the two-dimensional (2D) plane $\tilde{A}(x)$, whose axes are u and $\mu_{\tilde{A}}(x,u)$, is called a *vertical slice* [20]; it is a T1 FS whose MF is called a *secondary MF*, i.e.,

$$\mu_{\tilde{A}(x)}(u) = \bigcup_{u\in[0,1]} \mu_{\tilde{A}}(x,u)/u. \tag{3}$$

The *support of the secondary MF* is $I_x = \{u \in [0,1]|\mu_{\tilde{A}}(x,u) > 0\}$. Depending upon whether or not I_x is connected (i.e., closed, open, or neither), an IT2 FS can assume different forms [3]. Because existing similarity measures for IT2 FSs have so far only been developed for closed I_x, *in this paper, we assume that I_x is closed*. More specifically, I_x is always an interval (or a single number, which is a special case of an interval). The extensions of the results in this paper to more general kinds of IT2 FSs (and GT2 FSs) are proposed as future research topics in Section VI.

When I_x is closed, it can be described as

$$I_x = [\underline{\mu}_{\tilde{A}}(x), \bar{\mu}_{\tilde{A}}(x)] \tag{4}$$

where

$$\underline{\mu}_{\tilde{A}}(x) = \inf\{u|u \in [0,1], \mu_{\tilde{A}}(x,u) > 0\} \tag{5}$$

$$\bar{\mu}_{\tilde{A}}(x) = \sup\{u|u \in [0,1], \mu_{\tilde{A}}(x,u) > 0\} \tag{6}$$

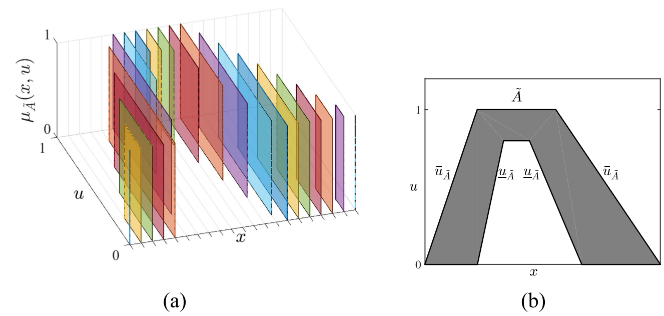

Fig. 1. Different representations of an IT2 FS. (a) Vertical slice representation. (b) Two-dimensional representation.

$\underline{\mu}_{\tilde{A}}(x)$ and $\bar{\mu}_{\tilde{A}}(x)$ are called the *lower* and *upper MFs* of the *footprint of uncertainty* (FOU) of $\tilde{A}$, FOU($\tilde{A}$), i.e.,

$$\text{FOU}(\tilde{A}) = \{(x,u)|x \in X \text{ and } u \in [\underline{\mu}_{\tilde{A}}(x), \bar{\mu}_{\tilde{A}}(x)]\}. \tag{7}$$

Any T1 FS within the FOU is called an *embedded T1 FS*. $\underline{\mu}_{\tilde{A}}(x)$ and $\bar{\mu}_{\tilde{A}}(x)$ are also embedded T1 FSs.

An IT2 FS using the vertical slice representation is shown in Fig. 1(a). Observe that all vertical slices have height 1 because $\mu_{\tilde{A}}(x,u) = 1$ for an IT2 FS. The FOU of an IT2 FS conveys all of the useful information about that FS and is easier to draw because it is 2-D. The FOU of the IT2 FS in Fig. 1(a) is shown Fig. 1(b).

B. Closed GT2 FSs

A GT2 FS [20], [21] $\tilde{A}$ is also represented by (2), but now $\mu_{\tilde{A}}(x,u)$ can be any value in $[0,1]$, instead of always being 1 as it is in an IT2 FS. The vertical slice representation of a GT2 FS is shown in Fig. 2(a). Here, the secondary MF for each x is an isosceles trapezoid, chosen only for ease of plotting.

A GT2 FS can also be represented by α-planes [22], or zSlices [30], as shown in Fig. 2(b). These two concepts are very similar.[2] In this paper, we use the α-plane terminology.

In the following, we assume that a GT2 FS is *closed*, which means that all of its α-planes are closed for $\alpha \in [0,1]$. This occurs when the α-cuts of all of the secondary MFs of $\tilde{A}$ are closed. Such secondary MFs do not have to be normal, and they may have either one apex (e.g., a triangle) or a collection of adjacent apexes, all of the same membership grade (e.g., a trapezoid). It is, therefore, to be understood that "GT2 FS" always mean "closed GT2 FSs" in this paper.

Let the α-cut [16] on the secondary MF $\tilde{A}(x)$ be

$$\tilde{A}(x)_\alpha = \{u|\mu_{\tilde{A}(x)}(u) \geq \alpha\} \equiv [a_\alpha(x), b_\alpha(x)]. \tag{8}$$

Then, the α-plane $\tilde{A}_\alpha$ is

$$\tilde{A}_\alpha = \bigcup_{x\in X} \tilde{A}(x)_\alpha/x = \bigcup_{x\in X} [a_\alpha(x), b_\alpha(x)]/x \tag{9}$$

[2][20, Table 6.2] compares the α-plane and zSlice descriptions. [20] also recommends using *horizontal slices* to denote them because it complements vertical slices and wavy slices [21] (another popular representation of GT2 and IT2 FSs; the wavy slice representation is not introduced in this paper because it is not needed here).

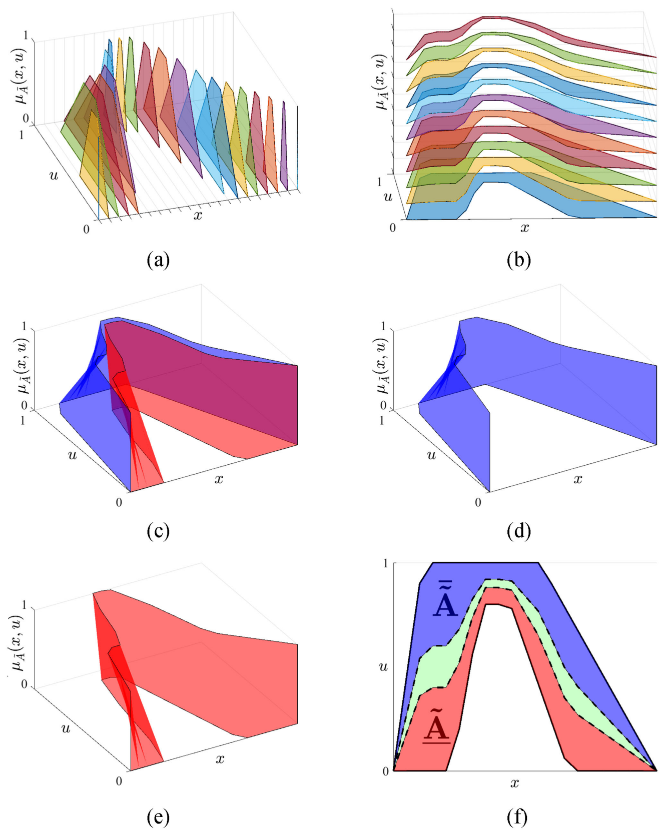

Fig. 2. Different representations of a closed GT2 FS. (a) Vertical slice representation. (b) α-plane, zSlice, or horizontal slice representation. (c) Surface representation in 3-D. (d) Upper surface. (e) Lower surface. (f) Surface representation in 2-D.

and the α-plane representation of $\tilde{A}$ is

$$\tilde{A} = \bigcup_{\alpha \in [0,1]} \alpha / \tilde{A}_\alpha. \tag{10}$$

In this paper, we also introduce a *surface representation* of GT2 FSs, as shown in Fig. 2(c). A GT2 FS $\tilde{A}$ is bounded from the outside by an *upper surface* $\bar{\tilde{A}}$ [shown in red in Fig. 2(c), and also separately in Fig. 2(d)] and by a *lower surface* $\underline{\tilde{A}}$ [shown in blue in Fig. 2(c), and also separately in Fig. 2(e)].

In terms of the vertical slice representation, the lower (upper) surface is spanned by the portion of the vertical slices that have smaller (larger) u than their corresponding apexes, i.e.,

$$\underline{\tilde{A}} = \bigcup_{x \in X} \bigcup_{u \in [a_0(x), a_1(x)]} \mu_{\tilde{A}}(x,u)/(x,u) \tag{11}$$

$$\bar{\tilde{A}} = \bigcup_{x \in X} \bigcup_{u \in [b_1(x), b_0(x)]} \mu_{\tilde{A}}(x,u)/(x,u). \tag{12}$$

In terms of the α-plane representation, the lower (upper) surface is spanned by all lower membership functions (LMFs) (upper membership functions—UMFs) of different α-planes, i.e.,

$$\underline{\tilde{A}} = \bigcup_{\alpha \in [0,1]} \bigcup_{x \in X} \alpha / (x, a_\alpha(x)) \tag{13}$$

$$\bar{\tilde{A}} = \bigcup_{\alpha \in [0,1]} \bigcup_{x \in X} \alpha / (x, b_\alpha(x)). \tag{14}$$

In practice, it is much more complicated to construct GT2 FSs [28] than T1 or IT2 FSs [35]. For convenience, frequently, the secondary MF for each x is chosen as an isosceles trapezoid, as shown in Fig. 2(a). Such GT2 FSs can also be conveniently plotted in 2-D, as in Fig. 2(f). The solid curves represent the boundary of $\tilde{A}_0$, and the light green area represents $\tilde{A}_1$. The α-planes in-between are interpolated linearly. The blue and red shades in Fig. 2(f) are the projections of the upper and lower surfaces in Fig. 2(c) into the xu plane, respectively.

III. Existing Similarity Measures for Closed GT2 FSs

This section gives a comprehensive overview of existing similarity measures for closed GT2 FSs, in the order of the year they were proposed. Their main formulas are summarized in Table I, and the details are explained in the following subsections. To the best of our knowledge, no similarity measures have been published for nonclosed GT2 FSs (as of August 2017).

Similarity of $\tilde{A}$ and $\tilde{B}$ makes use of $\tilde{A}(x)_\alpha$ in (9) and $\tilde{B}(x)_\alpha$, where

$$\tilde{B}(x)_\alpha = \{u | \mu_{\tilde{B}(x)}(u) \geq \alpha\} \equiv [c_\alpha(x), d_\alpha(x)]. \tag{15}$$

A. Hung and Yang's (HY) Similarity Measure

Hung and Yang [13] proposed two similarity measures for GT2 FSs in 2004.

Let U and V be crisp sets, and U^λ and V^λ be the crisp points within distance λ of them, respectively, i.e., if $U = [l, r]$, then $U^\lambda = [l - \lambda, r + \lambda]$. The Hausdorff distance between U and V is defined as

$$H(U,V) = \max\{L(U,V), L(V,U)\} \tag{16}$$

where

$$L(U,V) = \inf\{\lambda \geq 0 | V \subset U^\lambda\}. \tag{17}$$

Let A and B be two T1 FSs, and A_{α_j} and B_{α_j} be their α-cuts at $\alpha = \alpha_j$ $(j = 1, \ldots, m)$, respectively. Then, the Hausdorff distance between A and B is defined as [6]

$$d_H(A,B) = \frac{\sum_{j=1}^m \alpha_j H(A_{\alpha_j}, B_{\alpha_j})}{\sum_{i=1}^m \alpha_j}. \tag{18}$$

Define the distance between two GT2 FSs $\tilde{A}$ and $\tilde{B}$ as [17]

$$d(\tilde{A}, \tilde{B}) = \frac{1}{n} \sum_{i=1}^n d_H(\tilde{A}(x_i), \tilde{B}(x_i)). \tag{19}$$

Then, Hung and Yang's [13] first similarity measure for GT2 FSs is

$$s_{\text{HY},1}(\tilde{A}, \tilde{B}) = 1 - d(\tilde{A}, \tilde{B}). \tag{20}$$

TABLE I
SIMILARITY MEASURES OF CLOSED GT2 FSS

Authors	Formula
Hung and Yang (HY) [13]	$s_{HY,1}(\tilde{A},\tilde{B}) = 1 - d(\tilde{A},\tilde{B})$
Hung and Yang (HY) [13]	$s_{HY,2}(\tilde{A},\tilde{B}) = 1 - \frac{1-\exp(-d(\tilde{A},\tilde{B}))}{1-\exp(-1)}$
Mitchell (M) [24]	$s_M(\tilde{A},\tilde{B}) = \frac{\sum_{j=1}^M \sum_{k=1}^N w_{jk}\cdot s(A_j^e,B_k^e)}{\sum_{j=1}^M \sum_{k=1}^N w_{jk}}$
Yang and Lin (YL) [38]	$s_{YL}(\tilde{A},\tilde{B}) = \frac{1}{n}\sum_{i=1}^n \frac{\sum_{j=1}^m \min\{u_j\cdot\mu_{\tilde{A}}(x_i,u_j),u_j\cdot\mu_{\tilde{B}}(x_i,u_j)\}}{\sum_{j=1}^m \max\{u_j\cdot\mu_{\tilde{A}}(x_i,u_j),u_j\cdot\mu_{\tilde{B}}(x_i,u_j)\}}$
Hwang, Yang, Hung and Lee (HYHL) [14]	$s_{HYHL}(\tilde{A},\tilde{B}) = \min(I(\tilde{A},\tilde{B}), I(\tilde{B},\tilde{A}))$
McCulloch, Wagner and Aickelin (MWA) [19]	$s_{MWA}(\tilde{A},\tilde{B}) = \frac{\sum_{k\in p(\tilde{A},\tilde{B})}\alpha_k\cdot s_\lambda(\tilde{A}_{\alpha_k},\tilde{B}_{\alpha_k})}{\sum_{k\in p(\tilde{A},\tilde{B})}\alpha_k}$
Zhao, Xiao, Li and Deng (ZXLD) [42]	$s_{ZXLD}(\tilde{A},\tilde{B}) = \frac{1}{p}\sum_{k=1}^p \frac{\int_{x\in X}\min(a_{\alpha_k}(x),c_{\alpha_k}(x))dx+\int_{x\in X}\min(b_{\alpha_k}(x),d_{\alpha_k}(x))dx}{\int_{x\in X}\max(a_{\alpha_k}(x),c_{\alpha_k}(x))dx+\int_{x\in X}\max(b_{\alpha_k}(x),d_{\alpha_k}(x))dx}$
Hao and Mendel (HM) [12]	$s_{HM}(\tilde{A},\tilde{B}) = \frac{\sum_{k=1}^p \alpha_k\cdot s_J(\tilde{A}_{\alpha_k},\tilde{B}_{\alpha_k})}{\sum_{k=1}^p \alpha_k}$
McCulloch and Wagner (MW) [18]	$s_{MW}(\tilde{A},\tilde{B}) = \frac{\sum_{k\in p(\tilde{A},\tilde{B})}\alpha_k\cdot s(\tilde{A}_{\alpha_k},\tilde{B}_{\alpha_k})}{\sum_{k\in p(\tilde{A},\tilde{B})}\alpha_k}$
Wu and Mendel	$s_J(\tilde{A},\tilde{B}) = \frac{(\underline{\tilde{A}\cap\tilde{B}})_v+(\overline{\tilde{A}\cap\tilde{B}})_v}{(\underline{\tilde{A}\cup\tilde{B}})_v+(\overline{\tilde{A}\cup\tilde{B}})_v}$

Hung and Yang's [13] second similarity measure for GT2 FSs is

$$s_{\text{HY},2}(\tilde{A},\tilde{B}) = 1 - \frac{1-\exp(-d(\tilde{A},\tilde{B}))}{1-\exp(-1)}. \tag{21}$$

B. Mitchell's (M) Similarity Measure

Mitchell [24] proposed a similarity measure for GT2 FSs in 2005. Assume that the primary domain of GT2 FSs $\tilde{A}$ and $\tilde{B}$ has been discretized into n points $x_1,\ldots,x_n$. He first identified $\tilde{A}_0$ and M random embedded T1 FSs $\{A_j^e\}_{j=1,\ldots,M}$ within it. Similarly, he also identified N random embedded T1 FSs $\{B_k^e\}_{k=1,\ldots,N}$ within $\tilde{B}_0$. Next, he defined the similarity between $\tilde{A}$ and $\tilde{B}$ as a weighted average

$$s_M(\tilde{A},\tilde{B}) = \frac{\sum_{j=1}^M \sum_{k=1}^N w_{jk}\cdot s(A_j^e,B_k^e)}{\sum_{j=1}^M \sum_{k=1}^N w_{jk}} \tag{22}$$

where $s(A_j^e,B_k^e)$ can be any similarity measure between T1 FSs A_j^e and B_k^e, and w_{jk} is a weight equal to the t-norm of the secondary membership grades

$$\begin{aligned} w_{jk} = t\Big(&\mu_{\tilde{A}}(x_1,u_{A_j^e}(x_1)),\ldots,\mu_{\tilde{A}}(x_n,u_{A_j^e}(x_n)),\\ &\mu_{\tilde{B}}(x_1,u_{B_k^e}(x_1)),\ldots,\mu_{\tilde{B}}(x_n,u_{B_k^e}(x_n))\Big). \end{aligned} \tag{23}$$

C. Yang and Lin's (YL) Similarity Measures

Yang and Lin [38] proposed a similarity measure for GT2 FSs in 2009. Its discrete form is

$$\begin{aligned} &s_{\text{YL}}(\tilde{A},\tilde{B})\\ &= \frac{1}{n}\sum_{i=1}^n \frac{\sum_{j=1}^m \min\{u_j\cdot\mu_{\tilde{A}}(x_i,u_j),u_j\cdot\mu_{\tilde{B}}(x_i,u_j)\}}{\sum_{j=1}^m \max\{u_j\cdot\mu_{\tilde{A}}(x_i,u_j),u_j\cdot\mu_{\tilde{B}}(x_i,u_j)\}} \end{aligned} \tag{24}$$

where u_j, $j=1,\ldots,m$, are uniformly located in $[0,1]$.

D. Hwang, Yang, Hung, and Lee's (HYHL) Similarity Measure

Hwang *et al.* [14] proposed a similarity measure for GT2 FSs in 2011. They first defined an inclusion measure

$$I(\tilde{A},\tilde{B}) = \frac{1}{\int_{x\in X}dx}\int_{x\in X} \frac{\min\{\int_{a_0(x)}^{b_0(x)}\mu_{\tilde{A}}(x)dm, \int_{c_0(x)}^{d_0(x)}\mu_{\tilde{B}}(x)dm\}}{\int_{a_0(x)}^{b_0(x)}\mu_{\tilde{A}}(x)dm}dx \tag{25}$$

where m is a fuzzy measure. Then, Hwang *et al.*'s similarity measure is

$$s_{\text{HYHL}}(\tilde{A},\tilde{B}) = \min(I(\tilde{A},\tilde{B}), I(\tilde{B},\tilde{A})). \tag{26}$$

Hwang *et al.* [14] showed that $s_{\text{HYHL}}(\tilde{A},\tilde{B})$ may be better than $s_{\text{HY},1}(\tilde{A},\tilde{B})$ and $s_{\text{YL}}(\tilde{A},\tilde{B})$. However, it is not clear how the fuzzy measure m can be determined, which hinders (26)'s wider adoption.

E. McCulloch, Wagner, and Aickelin's (MWA) Similarity Measure

McCulloch *et al.* [19] proposed a similarity measure for GT2 FSs in 2013 based on α-planes (zSlices)

$$s_{\text{MWA}}(\tilde{A},\tilde{B}) = \frac{\sum_{k\in r(\tilde{A},\tilde{B})}\alpha_k\cdot s_\lambda(\tilde{A}_{\alpha_k},\tilde{B}_{\alpha_k})}{\sum_{k\in r(\tilde{A},\tilde{B})}\alpha_k} \tag{27}$$

where $r(\tilde{A},\tilde{B}) = \{\alpha_k|\tilde{A}_{\alpha_k}\neq\emptyset, \text{or } \tilde{B}_{\alpha_k}\neq\emptyset\}$ is the union set of α in $\tilde{A}$ and $\tilde{B}$, and s_λ can be any similarity measure for IT2 FSs, e.g., the Jaccard similarity measure [33], or any of those summarized in [33, Sec. 4].

F. Zhao, Xiao, Li, and Deng's (ZXLD) Similarity Measure

Zhao *et al.* [42] proposed a similarity measure for GT2 FSs in 2014 based on α-planes. They first defined the similarity between two GT2 FSs as a T1 FS

$$\tilde{s}_{\text{ZXLD}}(\tilde{A},\tilde{B}) = \bigcup_{k=1}^{p} \left\{\alpha_k / \left[s_L(\tilde{A},\tilde{B},\alpha_k), s_R(\tilde{A},\tilde{B},\alpha_k)\right]\right\} \quad (28)$$

where

$$s_L(\tilde{A},\tilde{B},\alpha_k) = \min\left\{\frac{\int_{x\in X}\min(a_{\alpha_k}(x),c_{\alpha_k}(x))dx}{\int_{x\in X}\max(a_{\alpha_k}(x),c_{\alpha_k}(x))dx}, \frac{\int_{x\in X}\min(b_{\alpha_k}(x),d_{\alpha_k}(x))dx}{\int_{x\in X}\max(b_{\alpha_k}(x),d_{\alpha_k}(x))dx}\right\} \quad (29)$$

$$s_R(\tilde{A},\tilde{B},\alpha_k) = \min\left\{\frac{\int_{x\in X}\min(a_{\alpha_k}(x),c_{\alpha_k}(x))dx}{\int_{x\in X}\max(a_{\alpha_k}(x),c_{\alpha_k}(x))dx}, \frac{\int_{x\in X}\min(b_{\alpha_k}(x),d_{\alpha_k}(x))dx}{\int_{x\in X}\max(b_{\alpha_k}(x),d_{\alpha_k}(x))dx}\right\}. \quad (30)$$

They then computed a crisp similarity measure[3] from $\tilde{s}_{\text{ZXLD}}(\tilde{A},\tilde{B})$ as $s_{\text{ZXLD}}(\tilde{A},\tilde{B})$ in Table I. Observe that $s_{\text{ZXLD}}(\tilde{A},\tilde{B})$ is actually the average of the Jaccard similarity measures for different α-planes.

G. Hao and Mendel's (HM) Similarity Measure

Hao and Mendel [12] proposed a similarity measure for GT2 FSs in 2014 based on α-planes. They first defined the similarity as a T1 FS

$$\tilde{s}_{\text{HM}}(\tilde{A},\tilde{B}) = \bigcup_{k=1}^{p} \alpha_k / s_J(\tilde{A}_{\alpha_k},\tilde{B}_{\alpha_k}) \quad (31)$$

where $s_J(\tilde{A}_{\alpha_k},\tilde{B}_{\alpha_k})$ is the Jaccard similarity measure between two IT2 FSs [33].

A crisp similarity measure can then be obtained as [12]

$$s_{\text{HM}}(\tilde{A},\tilde{B}) = \frac{\sum_{k=1}^{p}\alpha_k \cdot s_J(\tilde{A}_{\alpha_k},\tilde{B}_{\alpha_k})}{\sum_{k=1}^{p}\alpha_k}. \quad (32)$$

Observe that $s_{\text{HM}}(\tilde{A},\tilde{B})$ is essentially the same as $s_{\text{MWA}}(\tilde{A},\tilde{B})$ in (27), when the Jaccard similarity measure for IT2 FSs is used as s_λ in (27).

H. McCulloch and Wagner's (MW) Similarity Measure

McCulloch and Wagner [18] proposed a similarity measure for GT2 FSs in 2016, based on α-planes (zSlices)

$$s_{\text{MW}}(\tilde{A},\tilde{B}) = \frac{\sum_{k\in r(\tilde{A},\tilde{B})}\alpha_k \cdot s(\tilde{A}_{\alpha_k},\tilde{B}_{\alpha_k})}{\sum_{k\in r(\tilde{A},\tilde{B})}\alpha_k} \quad (33)$$

where $r(\tilde{A},\tilde{B}) = \{\alpha_k | \tilde{A}_{\alpha_k} \neq \emptyset, \text{or } \tilde{B}_{\alpha_k} \neq \emptyset\}$ is again the union set of α in $\tilde{A}$ and $\tilde{B}$, as explained for $s_{\text{MWA}}(\tilde{A},\tilde{B})$, and s is a similarity measure for IT2 FSs

$$s(\tilde{A}_{\alpha_k},\tilde{B}_{\alpha_k}) = \begin{cases} s_\lambda(\tilde{A}_{\alpha_k},\tilde{B}_{\alpha_k}), & \tilde{A}_{\alpha_k} \neq \emptyset \text{ and } \tilde{B}_{\alpha_k} \neq \emptyset \\ 0, & \text{otherwise.} \end{cases} \quad (34)$$

Observe that the only difference between $s_{\text{MW}}(\tilde{A},\tilde{B})$ and $s_{\text{MWA}}(\tilde{A},\tilde{B})$ is the similarity measure for IT2 FSs used in them. When the secondary MFs of $\tilde{A}$ and/or $\tilde{B}$ do not have equal heights, $\tilde{A}_{\alpha_k} = \emptyset$ or $\tilde{B}_{\alpha_k} = \emptyset$ for certain α_k, and $s_\lambda(\tilde{A}_{\alpha_k},\tilde{B}_{\alpha_k})$ in (27) is undefined; however, $s(\tilde{A}_{\alpha_k},\tilde{B}_{\alpha_k})$ in (34) is defined (equals 0), so $s_{\text{MW}}(\tilde{A},\tilde{B})$ can handle GT2 FSs whose secondary MFs may have different heights or be subnormal, whereas $s_{\text{MWA}}(\tilde{A},\tilde{B})$ cannot.

IV. Jaccard Similarity Measure for GT2 FSs

This section points out the limitations of existing similarity measures for GT2 FSs, proposes a geometric explanation of the popular Jaccard similarity measure for T1 and IT2 FSs, and extends it to GT2 FSs. It also shows that the Jaccard similarity measure for GT2 FSs satisfies the four properties of a similarity measure proposed in [32] and [33].

A. Limitations of Existing Similarity Measures for GT2 FSs

Nine existing similarity measures for GT2 FSs have been introduced in the previous section. Among them, Mitchell's similarity measure is special because it involves random sampling. As a result, its output is not deterministic, and generally, $s_M(\tilde{A},\tilde{A}) \neq 1$, both of which are counterintuitive. The other eight similarity measures all utilize some slices in their computation.

1) The HY, YL, and HYHL similarity measures first cut the two GT2 FSs into vertical slices at different x, then compute the similarity (or distance) between each vertical slice pair (which belongs to the same x), and, finally, aggregate these similarities (or distances).
2) The MWA, ZXLD, HM, and MW similarity measures first cut the two GT2 FSs into α-planes at different α, then compute the similarity between each α-plane pair (which belongs to the same α), and, finally, aggregate these similarities.

Fig. 2 shows that each GT2 FS can be represented equivalently by vertical slices or α-planes, so, theoretically, the similarity measure between two GT2 FSs should be computed equivalently using both vertical slices and α-planes, as we pointed out in Section I. Unfortunately, none of the existing similarity measures for GT2 FSs can be computed using both slices: each of them is exclusive to a specific representation and cannot be computed using the other representation. The HY, YL, and HYHL similarity measures cannot be computed using the α-plane representation, and the MWA, ZXLD, HM, and MW similarity measures cannot be computed using the vertical slice representation. So, next, we propose a geometry-based similarity measure for GT2 FSs that gives the same result whether it is computed using the vertical slices or α-planes.

[3]Though Zhao *et al.* [42] claimed that $s_{\text{ZXLD}}(\tilde{A},\tilde{B})$ in Table I is the centroid of $\tilde{s}_{\text{ZXLD}}(\tilde{A},\tilde{B})$, actually it is not. And the connection between $\tilde{s}_{\text{ZXLD}}(\tilde{A},\tilde{B})$ and $s_{\text{ZXLD}}(\tilde{A},\tilde{B})$ was not explained clearly in [42].

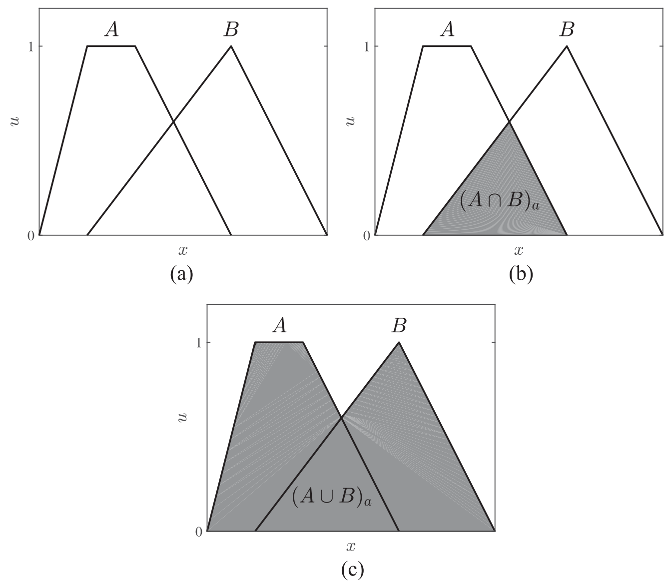

Fig. 3. Geometric illustration of the Jaccard similarity for T1 FSs: the area perspective. (a) A and B. (b) $(A \cap B)_a$. (c) $(A \cup B)_a$.

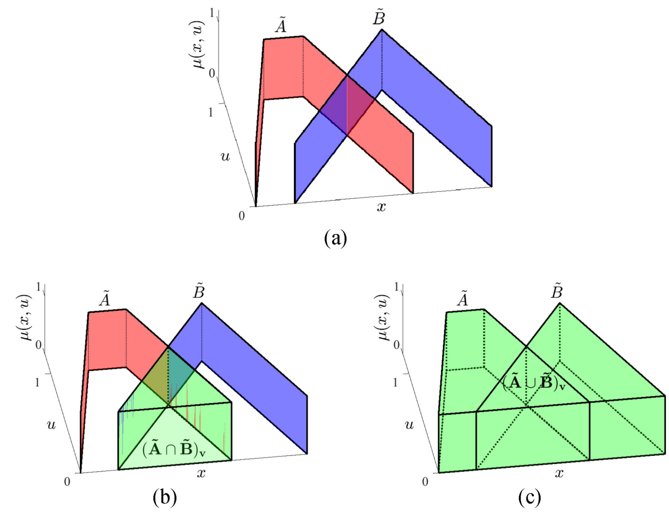

Fig. 4. Geometric illustration of the Jaccard similarity for T1 FSs: the volume perspective. (a) $\tilde{A}$ and $\tilde{B}$. (b) $(\tilde{A} \cap \tilde{B})_v$ as the green volume. (c) $(\tilde{A} \cup \tilde{B})_v$ as the green volume.

B. Jaccard Similarity Measure for T1 FSs

The Jaccard similarity measure for T1 FSs, arguably the most widely used such similarity measure, is [15]

$$s_{J,T1}(A, B) = \frac{\sum_{i=1}^{n} \min(u_A(x_i), u_B(x_i))}{\sum_{i=1}^{n} \max(u_A(x_i), u_B(x_i))}. \tag{35}$$

Interestingly, this similarity measure can be understood geometrically by viewing each T1 FS as an area in the 2-D plane of x and u, as shown in Fig. 3(a). Let $(A \cap B)_a$ be the common area of A and B, as shown in Fig. 3(b), and $(A \cup B)_a$ be the area of their union, as shown in Fig. 3(c). Then, $s_{J,T1}(A, B)$ above equals the ratio of the common area to the union area (when integrals are discretized), i.e.,

$$s^a_{J,T1}(A, B) = \frac{(A \cap B)_a}{(A \cup B)_a}. \tag{36}$$

A T1 FS A can also be viewed as a special GT2 FS $\tilde{A}$

$$\tilde{A} = \int_{x \in X} 1/(x, u_A(x)) \tag{37}$$

as shown in Fig. 4(a). Let $(\tilde{A} \cap \tilde{B})_v$ be the common volume of $\tilde{A}$ and $\tilde{B}$, which is a triangular prism with height 1, shown as the shape shaded in green in Fig. 4(b). Let $(\tilde{A} \cup \tilde{B})_v$ be the volume of the union of $\tilde{A}$ and $\tilde{B}$, which is a column with height 1, shown as the shape shaded in green in Fig. 4(c). Because the triangular prism has height 1, numerically $(\tilde{A} \cap \tilde{B})_v = (A \cap B)_a$. Similarly, numerically, $(\tilde{A} \cup \tilde{B})_v = (A \cup B)_a$. So, from the volume perspective, we can re-express the Jaccard similarity measure as

$$s^v_{J,T1}(\tilde{A}, \tilde{B}) = \frac{(\tilde{A} \cap \tilde{B})_v}{(\tilde{A} \cup \tilde{B})_v}, \tag{38}$$

which is the ratio of the common volume to the union volume. It is easy to see that $s^v_{J,T1}(\tilde{A}, \tilde{B})$ equals $s^a_{J,T1}(A, B)$.

C. Jaccard Similarity Measure for IT2 FSs

The Jaccard similarity measure for two IT2 FSs can also be understood from the area perspective and the volume perspective.

When we ignore the secondary membership grades of an IT2 FS $\tilde{A}$, it can be plotted in the 2-D space of x and u and bounded from above and below by T1 FSs $\bar{u}_{\tilde{A}}$ and $\underline{u}_{\tilde{A}}$, as shown in Fig. 1(b). By considering both shape and proximity information, the Jaccard similarity measure for two IT2 FSs $\tilde{A}$ and $\tilde{B}$, that is defined in [33], can be interpreted from the area perspective as

$$s^a_{J,IT2}(\tilde{A}, \tilde{B}) = \frac{(\underline{u}_{\tilde{A}} \cap \underline{u}_{\tilde{B}})_a + (\bar{u}_{\tilde{A}} \cap \bar{u}_{\tilde{B}})_a}{(\underline{u}_{\tilde{A}} \cup \underline{u}_{\tilde{B}})_a + (\bar{u}_{\tilde{A}} \cup \bar{u}_{\tilde{B}})_a} \tag{39}$$

where $(\underline{u}_{\tilde{A}} \cap \underline{u}_{\tilde{B}})_a$ is the common area of $\underline{u}_{\tilde{A}}$ and $\underline{u}_{\tilde{B}}$, $(\bar{u}_{\tilde{A}} \cap \bar{u}_{\tilde{B}})_a$ is the common area of $\bar{u}_{\tilde{A}}$ and $\bar{u}_{\tilde{B}}$, $(\underline{u}_{\tilde{A}} \cup \underline{u}_{\tilde{B}})_a$ is the area of the union of $\underline{u}_{\tilde{A}}$ and $\underline{u}_{\tilde{B}}$, and $(\bar{u}_{\tilde{A}} \cap \bar{u}_{\tilde{B}})_a$ is the area of the union of $\bar{u}_{\tilde{A}}$ and $\bar{u}_{\tilde{B}}$. In short, $s^a_{J,IT2}(\tilde{A}, \tilde{B})$ is the ratio of the average common area of the intersections of the lower and upper surfaces to the corresponding average common area of their unions.

From the volume perspective, the Jaccard similarity measure for two IT2 FSs $\tilde{A}$ and $\tilde{B}$ can be re-expressed as

$$s^v_{J,IT2}(\tilde{A}, \tilde{B}) = \frac{(\underline{\tilde{A}} \cap \underline{\tilde{B}})_v + (\bar{\tilde{A}} \cap \bar{\tilde{B}})_v}{(\underline{\tilde{A}} \cup \underline{\tilde{B}})_v + (\bar{\tilde{A}} \cup \bar{\tilde{B}})_v} \tag{40}$$

where $(\underline{\tilde{A}} \cap \underline{\tilde{B}})_v$ is the common volume of the two lower surfaces $\underline{\tilde{A}}$ and $\underline{\tilde{B}}$, and $(\underline{\tilde{A}} \cup \underline{\tilde{B}})_v$ is the volume of their union. $(\underline{\tilde{A}} \cap \underline{\tilde{B}})_v$ and $(\bar{\tilde{A}} \cap \bar{\tilde{B}})_v$ can be computed similarly to that in Fig. 4(b), and $(\underline{\tilde{A}} \cup \underline{\tilde{B}})_v$ and $(\bar{\tilde{A}} \cup \bar{\tilde{B}})_v$ can be computed similarly to that in Fig. 4(c). Each of $(\underline{\tilde{A}} \cap \underline{\tilde{B}})_v$, $(\bar{\tilde{A}} \cap \bar{\tilde{B}})_v$, $(\underline{\tilde{A}} \cup \underline{\tilde{B}})_v$, and $(\bar{\tilde{A}} \cup \bar{\tilde{B}})_v$ is a column with height 1, so, numerically, we have $(\underline{\tilde{A}} \cap \underline{\tilde{B}})_v = (\underline{u}_{\tilde{A}} \cap \underline{u}_{\tilde{B}})_a$, $(\bar{\tilde{A}} \cap \bar{\tilde{B}})_v = (\bar{u}_{\tilde{A}} \cap \bar{u}_{\tilde{B}})_a$,

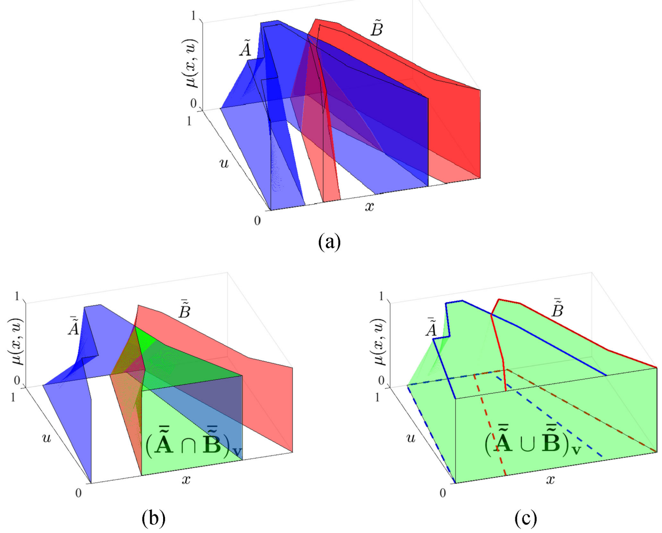

Fig. 5. Geometric illustration of the Jaccard similarity for GT2 FSs. (a) $\tilde{A}$ and $\tilde{B}$. (b) $(\bar{\tilde{A}} \cap \bar{\tilde{B}})_v$. (c) $(\bar{\tilde{A}} \cup \bar{\tilde{B}})_v$.

$(\underline{\tilde{A}} \cup \underline{\tilde{B}})_v = (\underline{u}_{\tilde{A}} \cup \underline{u}_{\tilde{B}})_a$, and $(\bar{\tilde{A}} \cup \bar{\tilde{B}})_v = (\bar{u}_{\tilde{A}} \cup \bar{u}_{\tilde{B}})_a$, i.e., $s^v_{J,IT2}(\tilde{A}, \tilde{B}) = s^a_{J,IT2}(\tilde{A}, \tilde{B})$.

D. Jaccard Similarity Measure for GT2 FSs

From the previous two subsections, we see that the Jaccard similarity measure for T1 and IT2 FSs can be understood from an area perspective and a volume perspective, and they give equivalent results. However, a GT2 FS is always 3-D (the secondary MF cannot be ignored), so, for it, we can only use the volume perspective.

We formally define the Jaccard similarity measure for GT2 FSs as

$$s_J(\tilde{A}, \tilde{B}) \equiv \frac{(\underline{\tilde{A}} \cap \underline{\tilde{B}})_v + (\bar{\tilde{A}} \cap \bar{\tilde{B}})_v}{(\underline{\tilde{A}} \cup \underline{\tilde{B}})_v + (\bar{\tilde{A}} \cup \bar{\tilde{B}})_v} \tag{41}$$

where $(\underline{\tilde{A}} \cap \underline{\tilde{B}})_v$ is the common volume of $\underline{\tilde{A}}$ and $\underline{\tilde{B}}$, $(\bar{\tilde{A}} \cap \bar{\tilde{B}})_v$ is the common volume of $\bar{\tilde{A}}$ and $\bar{\tilde{B}}$, as shown in Fig. 5(b), $(\underline{\tilde{A}} \cup \underline{\tilde{B}})_v$ is the volume of the union of $\underline{\tilde{A}}$ and $\underline{\tilde{B}}$, and $(\bar{\tilde{A}} \cup \bar{\tilde{B}})_v$ is the volume of the union of $\bar{\tilde{A}}$ and $\bar{\tilde{B}}$, as shown in Fig. 5(c).

Note that $s_J(\tilde{A}, \tilde{B})$ uses the surface representation depicted in Fig. 2(c). It is conceptually intuitive, but cannot be computed directly. To compute $s_J(\tilde{A}, \tilde{B})$, we need to translate the surface representation to either the vertical slice representation or the α-plane representation.

When the α-plane representation in (13) and (14) is used, $s_J(\tilde{A}, \tilde{B})$ can be computed using (42) shown at the bottom of this page. Using $\bar{\tilde{A}}$ and $\bar{\tilde{B}}$ shown in Fig. 5(c), we next illustrate why, e.g., $(\bar{\tilde{A}} \cup \bar{\tilde{B}})_v$ [the green volume in Fig. 5(c)] can be approximately computed by $\frac{|X|}{np} \sum_{k=1}^{p} \sum_{i=1}^{n} \max(b_{\alpha_k}(x_i), d_{\alpha_k}(x_i))$; however, the idea also holds for the other three terms in (42).

Let p be the number of equally spaced α in $[0, 1]$, and α_k be the kth α ($k = 1, \ldots, p$). Then, the light green volume in Fig. 5(c) is the sum of $p - 1$ subvolumes between the α_k and α_{k+1} planes ($k = 1, \ldots, p - 1$), respectively. Two such subvolumes for $k = 1$ and $k = 3$ ($p = 11$) are shown in Fig. 6(a) and (b), respectively. Let n be the number of equally spaced samples in the x domain, and x_i be the ith sample ($i = 1, \ldots, n$). Then, the primary membership grade of (x_i, α_1) on the intersection of the upper surfaces $\bar{\tilde{A}}$ and $\bar{\tilde{B}}$ is $\max(b_{\alpha_1}(x_i), d_{\alpha_1}(x_i))$, shown as the corresponding black line in the dark green region of Fig. 6(a). Geometrically, the dark green subvolume in Fig. 6(a) can be approximated by $\frac{|X|}{2n(p-1)} \sum_{i=1}^{n} [\max(b_{\alpha_1}(x_i), d_{\alpha_1}(x_i)) + \max(b_{\alpha_2}(x_i), d_{\alpha_2}(x_i))]$, and the dark green subvolume in Fig. 6(b) by $\frac{|X|}{2n(p-1)} \sum_{i=1}^{n} [\max(b_{\alpha_2}(x_i), d_{\alpha_2}(x_i)) + \max(b_{\alpha_3}(x_i), d_{\alpha_3}(x_i))]$. Consequently, the light green volume in Fig. 5(c), which is $(\bar{\tilde{A}} \cup \bar{\tilde{B}})_v$, can be approximated as

$$(\bar{\tilde{A}} \cup \bar{\tilde{B}})_v = \frac{|X|}{2n(p-1)} \sum_{k=1}^{p-1} \sum_{i=1}^{n} [\max(b_{\alpha_k}(x_i), d_{\alpha_k}(x_i)) + \max(b_{\alpha_{k+1}}(x_i), d_{\alpha_{k+1}}(x_i))]. \tag{44}$$

In practice, it is more convenient to write (44) as

$$(\bar{\tilde{A}} \cup \bar{\tilde{B}})_v = \frac{|X|}{np} \sum_{k=1}^{p} \sum_{i=1}^{n} \max(b_{\alpha_k}(x_i), d_{\alpha_k}(x_i)). \tag{45}$$

When p is large, (44) and (45) give almost identical outputs. When the same $\{x_i\}_{i=1}^n$ and $\{\alpha_k\}_{k=1}^p$ are used in all four terms of $s_J(\tilde{A}, \tilde{B})$, all of them have an identical scaling factor $\frac{|X|}{np}$, which can be canceled out. That is why, we can replace $(\bar{\tilde{A}} \cup \bar{\tilde{B}})_v$ in (41) by $\sum_{k=1}^{p} \sum_{i=1}^{n} \max(b_{\alpha_k}(x_i), d_{\alpha_k}(x_i))$ in (42).

When the same $\{\alpha_k\}_{k=1}^p$ and $\{x_i\}_{i=1}^n$ in the α-plane representation above are used in the vertical slice representation [(11) and (12)], $s_J(\tilde{A}, \tilde{B})$ can be computed using (43) shown at the bottom of this page. Using the $\bar{\tilde{A}}$ and $\bar{\tilde{B}}$ in Fig. 5(c), Fig. 7 illustrates why $(\bar{\tilde{A}} \cup \bar{\tilde{B}})_v$ can be represented by $\sum_{k=1}^{p} \sum_{i=1}^{n} \max(a_{\alpha_k}(x_i), c_{\alpha_k}(x_i))$ in (43) (scaling factor canceled out). The idea is that $(\bar{\tilde{A}} \cup \bar{\tilde{B}})_v$, the light green volume in Fig. 5(c), is the sum of the subvolumes corresponding to different vertical slices, two of which are shown in Fig. 7.

$$s_J(\tilde{A}, \tilde{B}) = \frac{\sum_{k=1}^{p} [\sum_{i=1}^{n} \min(a_{\alpha_k}(x_i), c_{\alpha_k}(x_i)) + \sum_{i=1}^{n} \min(b_{\alpha_k}(x_i), d_{\alpha_k}(x_i))]}{\sum_{k=1}^{p} [\sum_{i=1}^{n} \max(a_{\alpha_k}(x_i), c_{\alpha_k}(x_i)) + \sum_{i=1}^{n} \max(b_{\alpha_k}(x_i), d_{\alpha_k}(x_i))]} \tag{42}$$

$$s_J(\tilde{A}, \tilde{B}) = \frac{\sum_{i=1}^{n} [\sum_{k=1}^{p} \min(a_{\alpha_k}(x_i), c_{\alpha_k}(x_i)) + \sum_{k=1}^{p} \min(b_{\alpha_k}(x_i), d_{\alpha_k}(x_i))]}{\sum_{i=1}^{n} [\sum_{k=1}^{p} \max(a_{\alpha_k}(x_i), c_{\alpha_k}(x_i)) + \sum_{k=1}^{p} \max(b_{\alpha_k}(x_i), d_{\alpha_k}(x_i))]} \tag{43}$$

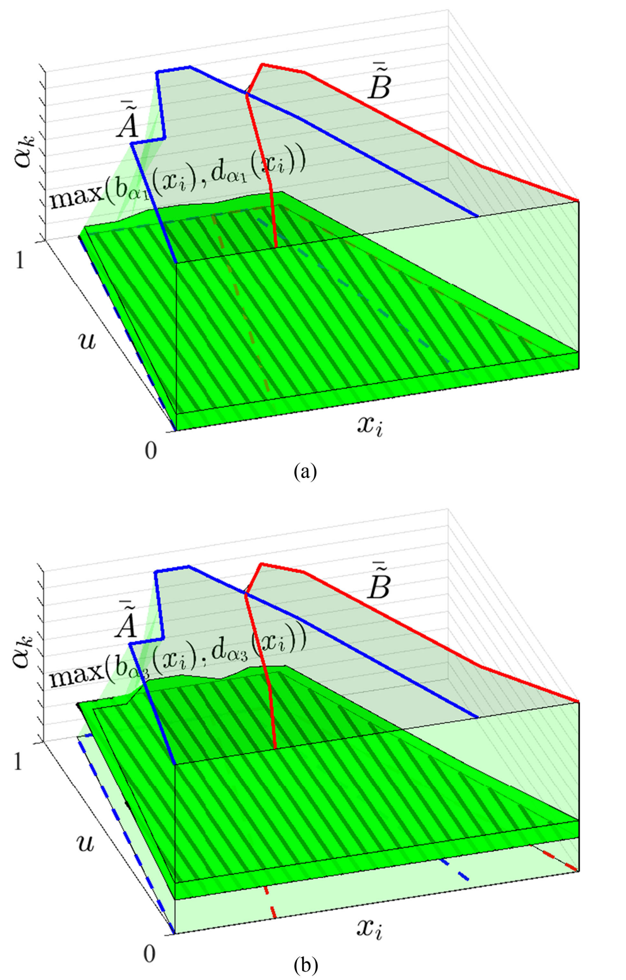

Fig. 6. Geometric illustration of the computation of $(\bar{\tilde{A}} \cup \bar{\tilde{B}})_v$ by α-planes. (a) Subvolume between $\alpha_1 = 0$ and $\alpha_2 = 0.1$ planes. (b) Subvolume between $\alpha_3 = 0.2$ and $\alpha_4 = 0.3$ planes.

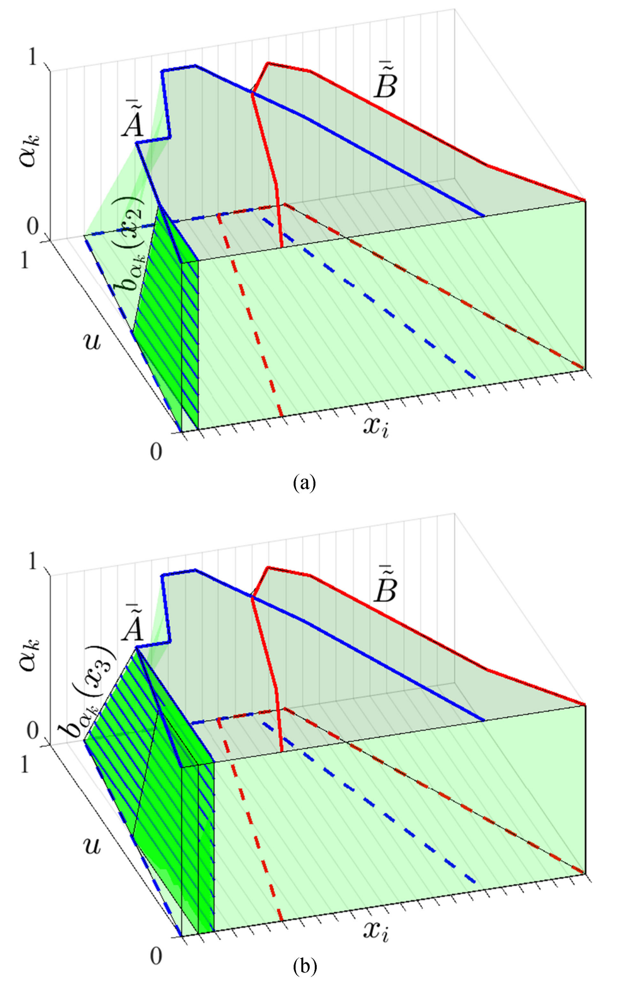

Fig. 7. Geometric illustration of the computation of $(\bar{\tilde{A}} \cup \bar{\tilde{B}})_v$ by vertical slices. (a) Subvolume between $x_1 = 0$ and x_2. (b) Subvolume between x_2 and x_3.

The following observations can be made from (42) and (43).

1) Equations (42) and (43) are equivalent.
2) When the GT2 FSs downgrade to IT2 or T1 FSs, the Jaccard similarity measure for GT2 FSs reduces to the corresponding Jaccard similarity measure for IT2 or T1 FSs.
3) Although $s_J(\tilde{A}, \tilde{B})$ in (42) looks similar to $s_{\text{ZXLD}}(\tilde{A}, \tilde{B})$ in Table I, they are not the same. $s_J(\tilde{A}, \tilde{B})$ in (42) is a ratio of volumes, and $s_{\text{ZXLD}}(\tilde{A}, \tilde{B})$ in Table I is an average of individual Jaccard similarity measures for different α-planes. Generally, these two quantities are not equal (although they may be close), as we will see in the next section. More importantly, the rationales behind these two definitions are fundamentally different.

E. Properties of $s_J(\tilde{A}, \tilde{B})$

When two real-world 3-D objects are compared by means of similarity, their proximity is not important, only their shape is important. For GT2 FSs (as well as for T1 and IT2 FSs), shape and proximity are both important, so any useful similarity measure for FSs must simultaneously handle shape and proximity. Motivated by this principle, the following four properties (requirements) of similarity measures for GT2 or IT2 FSs have been proposed in the literature [32], [33] and are used in this paper.

P1. *Reflexivity*: $s(\tilde{A}, \tilde{B}) = 1 \Leftrightarrow \tilde{A} = \tilde{B}$.
P2. *Symmetry*: $s(\tilde{A}, \tilde{B}) = s(\tilde{B}, \tilde{A})$.
P3. *Transitivity*[4]: If $\tilde{A} \le \tilde{B} \le \tilde{C}$, then $s(\tilde{A}, \tilde{B}) \ge s(\tilde{A}, \tilde{C})$.
P4. *Overlapping*[5]: If $\tilde{A} \cap \tilde{B} \ne \emptyset$, then $s(\tilde{A}, \tilde{B}) > 0$; otherwise, $s(\tilde{A}, \tilde{B}) = 0$.

The Jaccard similarity measure for T1 and IT2 FSs satisfy these four properties [33]. Similarly, we have the following theorem, whose proof is given in the Appendix.

Theorem 1: $s_J(\tilde{A}, \tilde{B})$ in (41) satisfies reflexivity, symmetry, transitivity, and overlapping. ■

[4] $\tilde{A} \le \tilde{B}$ if $\overline{\mu}_{\tilde{A}}(x, u) \le \overline{\mu}_{\tilde{B}}(x, u)$ and $\underline{\mu}_{\tilde{A}}(x, u) \le \underline{\mu}_{\tilde{B}}(x, u)$ for $\forall x$ and $\forall u$.

[5] $\tilde{A} \cap \tilde{B} \ne \emptyset$, i.e., $\tilde{A}$ and $\tilde{B}$ overlap, if $\exists x$ and $\exists u$ such that $\min(\overline{\mu}_{\tilde{A}}(x, u), \overline{\mu}_{\tilde{B}}(x, u)) > 0$. $\tilde{A} \cap \tilde{B} = \emptyset$, i.e., $\tilde{A}$ and $\tilde{B}$ do not overlap, if $\min(\overline{\mu}_{\tilde{A}}(x, u), \overline{\mu}_{\tilde{B}}(x, u)) = \min(\underline{\mu}_{\tilde{A}}(x, u), \underline{\mu}_{\tilde{B}}(x, u)) = 0$ $\forall x$ and $\forall u$.

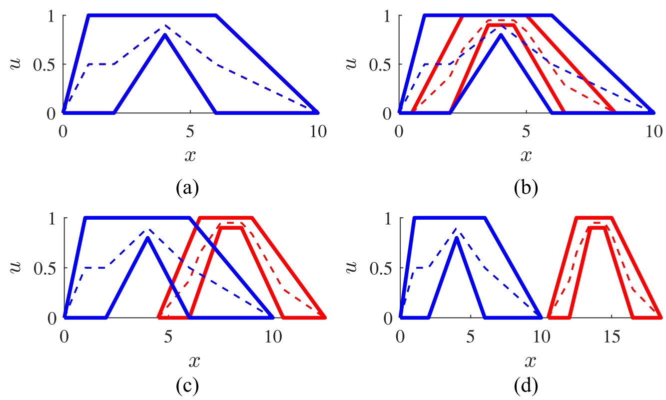

Fig. 8. (a)–(d) GT2 FSs used in Example 1. In each subfigure, the blue curves represent GT2 FS $\tilde{A}$, and the red curves $\tilde{B}$. For each GT2 FS, the solid blue or red curves represent the α-plane at $\alpha = 0$, and the dashed blue or red curves represent the corresponding α-plane at $\alpha = 1$. $\tilde{A}$ and $\tilde{B}$ are identical in (a).

TABLE II
SIMILARITIES OF THE GT2 FSS SHOWN IN FIG. 8, COMPUTED FROM DIFFERENT APPROACHES

	$s_{HY,1}$	$s_{HY,2}$	s_M	s_{YL}	s_{MWA} s_{MW} s_{HM}	s_{ZXLD}	s_J
Fig. 8(a)	1	1	.6454	1	1	1	1
Fig. 8(b)	.8165	.7348	.6112	.2433	.7161	.7092	.7091
Fig. 8(c)	.4650	.3445	.1640	.1896	.1775	.1773	.1773
Fig. 8(d)	.4739	.3528	0	.2486	0	0	0

V. EXAMPLES AND DISCUSSIONS

Two examples are presented in this section to compare the different similarity measures for GT2 FSs. Note that we do not include $s_{\rm HYHL}(\tilde{A}, \tilde{B})$ because it uses a fuzzy measure, but it is not clear how the fuzzy measure should be determined, so we were not able to implement it.

A. Example 1

In this example, we constructed $\tilde{A}$ as the blue GT2 FSs in Fig. 8, and $\tilde{B}$ as the red GT2 FSs. For each GT2 FS, the solid blue or red curves represent the α-plane at $\alpha = 0$, and the dashed blue or red curves represent the corresponding α-plane at $\alpha = 1$. The α-planes in-between were interpolated linearly. The dashed curves consist of the middle points of the LMFs and UMFs at $\alpha = 0$, i.e., $a_1(x) = b_1(x) = 0.5[a_0(x) + b_0(x)]$, meaning that the secondary MFs are all isosceles triangles.

The corresponding similarities between $\tilde{A}$ and $\tilde{B}$, computed from different approaches, are given in Table II. Observe the following.

1) $s_{\rm HY,1}$, $s_{\rm HY,2}$, and $s_{\rm YL}$ gave positive similarities even when $\tilde{A}$ and $\tilde{B}$ do not overlap at all, which is counterintuitive. Moreover, they all gave larger similarities for the two GT2 FSs shown in Fig. 8(d) than those two shown in Fig. 8(c), which is even more counterintuitive.
2) s_M gave a similarity of 0.6454 for identical $\tilde{A}$ and $\tilde{B}$ in Fig. 8(a), which is counterintuitive.

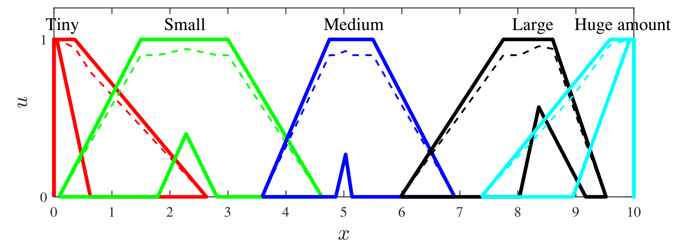

Fig. 9. GT2 FSs used in Example 2. The solid curves indicate the α-planes at $\alpha = 0$, and the dashed curves indicate the α-planes at $\alpha = 1$.

TABLE III
SIMILARITIES BETWEEN THE GT2 FSS SHOWN IN FIG. 9

		Tiny	Small	Medium	Large	Huge amount
$s_{HY,1}$	Tiny	1	.4364	.5203	.6335	.7094
	Small	.4364	1	.3631	.4841	.5681
	Medium	.5203	.3631	1	.3772	.4771
	Large	.6335	.4841	.3772	1	.4640
	Huge amount	.7094	.5681	.4771	.4640	1
$s_{HY,2}$	Tiny	1	.3184	.3972	.5146	.6010
	Small	.3184	1	.2548	.3624	.4452
	Medium	.3972	.2548	1	.2666	.3558
	Large	.5146	.3624	.2666	1	.3436
	Huge amount	.6010	.4452	.3558	.3436	1
s_M	Tiny	.6561	.1690	0	0	0
	Small	.1695	.5505	.0307	0	0
	Medium	0	.0307	.5144	.0250	0
	Large	0	0	.0250	.6051	.1813
	Huge amount	0	0	0	.1812	.7356
s_{YL}	Tiny	1	.2149	.3633	.5186	.5749
	Small	.2149	1	.3435	.4038	.4796
	Medium	.3633	.3435	1	.3268	.3009
	Large	.5186	.4038	.3268	1	.1270
	Huge amount	.5749	.4796	.3009	.1270	1
s_{MWA} s_{MW} s_{HM}	Tiny	1	.2296	0	0	0
	Small	.2296	1	.0386	0	0
	Medium	0	.0386	1	.0323	0
	Large	0	0	.0323	1	.2278
	Huge amount	0	0	0	.2278	1
s_{ZXLD}	Tiny	1	.2246	0	0	0
	Small	.2246	1	.0384	0	0
	Medium	0	.0384	1	.0319	0
	Large	0	0	.0319	1	.2193
	Huge amount	0	0	0	.2193	1
s_J	Tiny	1	.2257	0	0	0
	Small	.2257	1	.0384	0	0
	Medium	0	.0384	1	.0320	0
	Large	0	0	.0320	1	.2208
	Huge amount	0	0	0	.2208	1

3) $s_{\rm MWA}$, $s_{\rm MW}$, $s_{\rm HM}$, $s_{\rm ZXLD}$, and s_J all gave reasonable similarities, and their results were very close. In fact, $s_{\rm MWA}$, $s_{\rm MW}$, and $s_{\rm HM}$ are identical when both $\tilde{A}$ and $\tilde{B}$ have normal secondary MFs at every vertical slice, as can be established from their formulas in Table I.

B. Example 2

In this example, we picked five IT2 FS word models, which were distributed roughly uniformly in $[0, 10]$ and were constructed using the enhanced interval approach [35]. The FOUs of the five IT2 FSs were used as the $\alpha = 0$ α-plane, and the secondary MFs had their bases pinned to the LMF and UMF of the FOU to obtain GT2 FSs.

We constructed the secondary MF of the GT2 FSs as $a_1(x) = b_1(x) = 0.1a_0(x) + 0.9b_0(x)$, i.e., the apexes of the secondary MFs were much closer to the UMF of the $\alpha = 0$ α-plane than to the LMF. The α-planes at $\alpha = 1$ are shown in Fig. 9 as the dashed curves, and the resulting similarity measures are shown in Table III. Observe that $s_{\text{HY},1}$, $s_{\text{HY},2}$, s_M, and s_{YL} still gave the counterintuitive results as explained in the previous example. The results of s_{MWA}, s_{MW}, s_{HM}, s_{ZXLD}, and s_J were more reasonable and are again very close to each other.

C. Summary

From the above two examples, we can observe that s_J may be close to s_{MWA}, s_{MW}, s_{HM}, and s_{ZXLD}; however, s_J is constructed based on a fundamentally different principle than them: it uses the geometries of the surface representation, which can be translated to both the vertical slice and α-plane representations, and gives the same result regardless of which representation is used, whereas the others use the α-plane representation, and they cannot be computed using the vertical slice representation.

VI. Conclusion and Future Research

In this paper, we have given a comprehensive overview of existing similarity measures for GT2 FSs, pointed out their limitations, and proposed a new similarity measure for closed GT2 FSs. The latter is an extension of the popular Jaccard similarity measure for T1 and IT2 FSs to GT2 FSs, one that uses a novel geometric explanation. The fundamental difference between the proposed Jaccard similarity measure for GT2 FSs and all existing similarity measures is that the Jaccard similarity measure focuses on the overall geometries of two GT2 FSs and does not depend on a specific representation of them, whereas all existing similarity measures for GT2 FSs depend either on their vertical slice or α-plane representations. We have shown that the Jaccard similarity measure for GT2 FSs satisfies four properties of a similarity measure and demonstrated its reasonableness using two examples. The geometric approach proposed in this paper may also be useful in defining subsethood measures [25] and uncertainty measures [31], [41] for closed GT2 FSs, which is one of our future research directions.

As pointed out in Section II-A, an IT2 FS can assume different forms depending on how I_x is defined. Theoretically, a GT2 FS can also assume different forms depending on how I_x is defined. The one shown in Fig. 2, in which each α-plane is closed, and each vertical slice is T1 FS that has closed α-cuts (but is not necessarily normal), is to date the only form of GT2 FS that has appeared in the literature and used in practice. However, theoretically, GT2 FSs may also be nonclosed, as shown in Fig. 10 , where, in each subfigure, the shaded volumes belong to a single GT2 FS instead of two separate GT2 FSs.

When some α-cuts of the secondary MFs of $\tilde{A}$ and $\tilde{B}$ are not closed, those similarity measures based on α-planes (s_{MWA}, s_{MW}, s_{HM}, and s_{ZLD}) cannot be used because now some α-planes will be multi-IV FSs, and no similarity measures for such FSs exist. Whether or not the other four existing similarity measures ($s_{\text{HY},1}$, $s_{\text{HY},2}$, s_M, and s_{YL}) can be used for nonclosed GT2 FSs is unclear, but that is not important, because

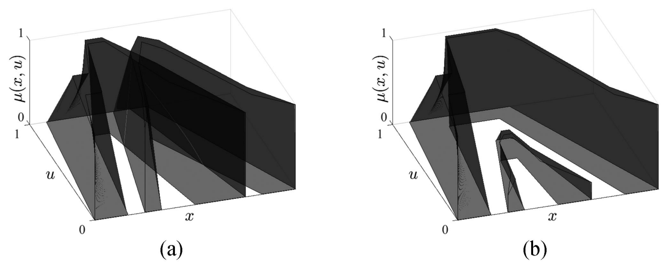

Fig. 10. Nonclosed GT2 FSs. (a) Each α-plane is a connected multi-IV FS, and some vertical slices consist of multiple intervals. (b) Each α-plane consists of multiple unconnected IV FSs, and each vertical slice consists of multiple intervals.

we have shown that they have other serious problems, so their results will not be good anyway. Our proposed Jaccard similarity measure in (41) cannot be used for such nonclosed GT2 FSs either because now it is difficult to define the upper and lower surfaces. So, another future research direction is to extend the similarity measures for closed GT2 FSs to nonclosed GT2 FSs. However, because similarity measures for GT2 FSs build upon similarity measures for IT2 FSs, we may need to develop similarity measures for nonclosed IT2 FSs first.

Finally, we defined the similarity measure for GT2 FSs as a crisp number in this paper, as, to our knowledge, almost all existing applications of similarity measures (such as those introduced in the second paragraph of Section I, except [9]) used only crisp similarity measures. However, theoretically, the similarity measure of GT2 FSs may also be defined as a T1 FS, which can capture more uncertainties and, hence, may be preferred in certain applications. How to define such a similarity measure for GT2 FSs using the geometric approach is also an interesting future research direction.

Appendix
Proof of Theorem 1

To simplify the proof, we rewrite (42) as (46) shown at the top of the next page. The four properties are proved next.

P1. *Reflexivity:* Consider first the necessity, i.e., $s_J(\tilde{A}, \tilde{B}) = 1 \Rightarrow \tilde{A} = \tilde{B}$. For GT2 FSs $\tilde{A}$ and $\tilde{B}$, $\min(a_{\alpha_k}(x_i), c_{\alpha_k}(x_i)) < \max(a_{\alpha_k}(x_i), c_{\alpha_k}(x_i))$; hence, the only way that $s_J(\tilde{A}, \tilde{B}) = 1$ is when $\min(a_{\alpha_k}(x_i), c_{\alpha_k}(x_i)) = \max(a_{\alpha_k}(x_i), c_{\alpha_k}(x_i))$ and $\min(b_{\alpha_k}(x_i), d_{\alpha_k}(x_i)) = \max(b_{\alpha_k}(x_i), d_{\alpha_k}(x_i))$, in which case $a_{\alpha_k}(x_i) = c_{\alpha_k}(x_i)$ and $b_{\alpha_k}(x_i) = d_{\alpha_k}(x_i)$, i.e., $\tilde{A} = \tilde{B}$.

Consider next the sufficiency, i.e., $\tilde{A} = \tilde{B} \Rightarrow s_J(\tilde{A}, \tilde{B}) = 1$. When $\tilde{A} = \tilde{B}$, i.e., $a_{\alpha_k}(x_i) = c_{\alpha_k}(x_i)$ and $b_{\alpha_k}(x_i) = d_{\alpha_k}(x_i)$, it follows that $\min((a_{\alpha_k}(x_i), c_{\alpha_k}(x_i)) = \max(a_{\alpha_k}(x_i), c_{\alpha_k}(x_i))$ and $\min(b_{\alpha_k}(x_i), d_{\alpha_k}(x_i)) = \max(b_{\alpha_k}(x_i), d_{\alpha_k}(x_i))$. Consequently, it follows from (46) that $s_J(\tilde{A}, \tilde{B}) = 1$.

P2. *Symmetry:* Observe from (46) that $s_J(\tilde{A}, \tilde{B})$ does not depend on the order of $\tilde{A}$ and $\tilde{B}$; so, $s_J(\tilde{A}, \tilde{B}) = s_J(\tilde{B}, \tilde{A})$.

P3. *Transitivity:* Denote the α-cut on the secondary MF $\tilde{C}(x)$ of GT2 FS $\tilde{C}$ as $\tilde{C}(x)_\alpha = \{u|\mu_{\tilde{C}(x)}(u) \geq \alpha\} \equiv$

$$s_J(\tilde{A},\tilde{B}) = \frac{\sum_{k=1}^{p}\sum_{i=1}^{n}[\min(a_{\alpha_k}(x_i),c_{\alpha_k}(x_i)) + \min(b_{\alpha_k}(x_i),d_{\alpha_k}(x_i))]}{\sum_{k=1}^{p}\sum_{i=1}^{n}[\max(a_{\alpha_k}(x_i),c_{\alpha_k}(x_i)) + \max(b_{\alpha_k}(x_i),d_{\alpha_k}(x_i))]} \quad (46)$$

$$s_J(\tilde{A},\tilde{B}) = \frac{\sum_{k=1}^{p}\sum_{i=1}^{n}[\min(a_{\alpha_k}(x_i),c_{\alpha_k}(x_i)) + \min(b_{\alpha_k}(x_i),d_{\alpha_k}(x_i))]}{\sum_{k=1}^{p}\sum_{i=1}^{n}[\max(a_{\alpha_k}(x_i),c_{\alpha_k}(x_i)) + \max(b_{\alpha_k}(x_i),d_{\alpha_k}(x_i))]} = \frac{\sum_{k=1}^{p}\sum_{i=1}^{n}[a_{\alpha_k}(x_i)+b_{\alpha_k}(x_i)]}{\sum_{k=1}^{p}\sum_{i=1}^{n}[c_{\alpha_k}(x_i)+d_{\alpha_k}(x_i)]} \quad (47)$$

$$s_J(\tilde{A},\tilde{C}) = \frac{\sum_{k=1}^{p}\sum_{i=1}^{n}[\min(a_{\alpha_k}(x_i),e_{\alpha_k}(x_i)) + \min(b_{\alpha_k}(x_i),f_{\alpha_k}(x_i))]}{\sum_{k=1}^{p}\sum_{i=1}^{n}[\max(a_{\alpha_k}(x_i),e_{\alpha_k}(x_i)) + \max(b_{\alpha_k}(x_i),f_{\alpha_k}(x_i))]} = \frac{\sum_{k=1}^{p}\sum_{i=1}^{n}[a_{\alpha_k}(x_i)+b_{\alpha_k}(x_i)]}{\sum_{k=1}^{p}\sum_{i=1}^{n}[e_{\alpha_k}(x_i)+f_{\alpha_k}(x_i)]} \quad (48)$$

$[e_\alpha(x), f_\alpha(x)]$. If $\tilde{A} \le \tilde{B} \le \tilde{C}$, then we have (47) and (48) shown at the top of this page.

Because $\tilde{B} \le \tilde{C}$, it follows that $\sum_{k=1}^{p}\sum_{i=1}^{n}[c_{\alpha_k}(x_i) + d_{\alpha_k}(x_i)] \le \sum_{k=1}^{p}\sum_{i=1}^{n}[e_{\alpha_k}(x_i) + f_{\alpha_k}(x_i)]$, and hence $s_J(\tilde{A},\tilde{B}) \ge s_J(\tilde{A},\tilde{C})$.

P4. *Overlapping:* If $\tilde{A}\cap\tilde{B} \ne \emptyset$, then $\exists x_i$ and $\exists \alpha_k$ such that $\min(b_{\alpha_k}(x_i), d_{\alpha_k}(x_i)) > 0$. So, the numerator of (46) is larger than 0, and the denominator of (46) is also larger than 0. Consequently, $s_J(\tilde{A},\tilde{B}) > 0$. On the other hand, when $\tilde{A}\cap\tilde{B} = \emptyset$, i.e., $\min(b_{\alpha_k}(x_i), d_{\alpha_k}(x_i)) = \min(a_{\alpha_k}(x_i), c_{\alpha_k}(x_i)) = 0$ for $\forall x_i$ and $\forall \alpha_k$, then the numerator of (46) becomes 0. Consequently, $s_J(\tilde{A},\tilde{B}) = 0$. ■

References

[1] H. Bustince, E. Barrenechea, and M. Pagola, "Restricted equivalence functions," *Fuzzy Sets Syst.*, vol. 157, no. 17, pp. 2333–2346, 2006.

[2] H. Bustince, E. Barrenechea, and M. Pagola, "Image thresholding using restricted equivalence functions and maximizing the measures of similarity," *Fuzzy Sets Syst.*, vol. 158, no. 5, pp. 496–516, 2007.

[3] H. Bustince, J. Fernandez, H. Hagras, F. Herrera, M. Pagola, and E. Barrenechea, "Interval type-2 fuzzy sets are generalization of interval-valued fuzzy sets: Toward a wider view on their relationship," *IEEE Trans. Fuzzy Syst.*, vol. 23, no. 5, pp. 1876–1882, Oct. 2015.

[4] K. S. Candan, W.-S. Li, and M. L. Priya, "Similarity-based ranking and query processing in multimedia databases," *Data Knowl. Eng.*, vol. 35, no. 3, pp. 259–298, 2000.

[5] O. Castillo and P. Melin, *Type-2 Fuzzy Logic Theory and Applications*. Berlin, Germany: Springer-Verlag, 2008.

[6] B. B. Chaudhuri and A. Rosenfeld, "A modified Hausdorff distance between fuzzy sets," *Inf. Sci.*, vol. 118, pp. 159–171, 1999.

[7] V. V. Cross and T. A. Sudkamp, *Similarity and Compatibility in Fuzzy Set Theory: Assessment and Applications*. Heidelberg, Germany: Physica-Verlag, 2002.

[8] C. Fu, A. Sarabakha, E. Kayacan, C. Wagner, R. John, and J. M. Garibaldi, "Novel, similarity-based non-singleton fuzzy logic control for improved uncertainty handling in quadrotor UAVs," in *Proc. IEEE Int. Conf. Fuzzy Syst.*, Naples, Italy, Jul. 2017, pp. 1–6.

[9] M. Galar, J. Fernandez, G. Beliakov, and H. Bustince, "Interval-valued fuzzy sets applied to stereo matching of color images," *IEEE Trans. Image Process.*, vol. 20, no. 7, pp. 1949–1961, Jul. 2011.

[10] H. Hagras, "A hierarchical type-2 fuzzy logic control architecture for autonomous mobile robots," *IEEE Trans. Fuzzy Syst.*, vol. 12, no. 4, pp. 524–539, Aug. 2004.

[11] H. Hagras, "Type-2 FLCs: A new generation of fuzzy controllers," *IEEE Comput. Intell. Mag.*, vol. 2, no. 1, pp. 30–43, Feb. 2007.

[12] M. Hao and J. M. Mendel, "Similarity measures for general type-2 fuzzy sets based on the α-plane representation," *Inf. Sci.*, vol. 277, pp. 197–215, 2014.

[13] W.-L. Hung and M.-S. Yang, "Similarity measures between type-2 fuzzy sets," *Int. J. Uncertainty, Fuzziness Knowl.-Based Syst.*, vol. 12, no. 6, pp. 827–841, 2004.

[14] C.-M. Hwang, M.-S. Yang, W.-L. Hung, and E. S. Lee, "Similarity, inclusion and entropy measures between type-2 fuzzy sets based on the Sugeno integral," *Math. Comput. Model.*, vol. 53, no. 9, pp. 1788–1797, 2011.

[15] P. Jaccard, "Nouvelles recherches sur la distribution florale," *Bull. Soc. Vaud des Sci. Naturelles*, vol. 44, p. 223, 1908.

[16] G. J. Klir and B. Yuan, *Fuzzy Sets and Fuzzy Logic: Theory and Applications*. Upper Saddle River, NJ, USA: Prentice-Hall, 1995.

[17] D. C. Lin and M. S. Yang, "A similarity measure between type-2 fuzzy sets with its application to clustering," in *Proc. 4th Int. Conf. Fuzzy Syst. Knowl. Discovery*, Haikou, China, Aug. 2007, pp. 726–731.

[18] J. McCulloch and C. Wagner, "Measuring the similarity between zSlices general type-2 fuzzy sets with non-normal secondary membership functions," in *Proc. IEEE Int. Conf. Fuzzy Syst.*, Vancouver, BC, Canada, Jul. 2016, pp. 461–468.

[19] J. McCulloch, C. Wagner, and U. Aickelin, "Extending similarity measures of interval type-2 fuzzy sets to general type-2 fuzzy sets," in *Proc. IEEE Int. Conf. Fuzzy Syst.*, Hyderabad, India, Jul. 2013, pp. 1–8.

[20] J. Mendel, *Uncertain Rule-Based Fuzzy Systems: Introduction and New Directions*, 2nd ed. New York, NY, USA: Springer, 2017.

[21] J. M. Mendel and R. I. John, "Type-2 fuzzy sets made simple," *IEEE Trans. Fuzzy Syst.*, vol. 10, no. 2, pp. 117–127, Apr. 2002.

[22] J. M. Mendel, F. Liu, and D. Zhai, "α-plane representation for type-2 fuzzy sets: Theory and applications," *IEEE Trans. Fuzzy Syst.*, vol. 17, no. 5, pp. 1189–1207, Oct. 2009.

[23] J. M. Mendel and D. Wu, *Perceptual Computing: Aiding People in Making Subjective Judgments*. Hoboken, NJ, USA: Wiley-IEEE Press, 2010.

[24] H. B. Mitchell, "Pattern recognition using type-II fuzzy sets," *Inf. Sci.*, vol. 170, nos. 2–4, pp. 409–418, 2005.

[25] J. T. Rickard, J. Aisbett, and G. Gibbon, "Fuzzy subsethood for fuzzy sets of type-2 and generalized type-n," *IEEE Trans. Fuzzy Syst.*, vol. 17, no. 1, pp. 50–60, Feb. 2009.

[26] M. Setnes, R. Babuska, U. Kaymak, H. R. Van, and N. Lemke, "Similarity measures in fuzzy rule base simplification," *IEEE Trans. Syst., Man, Cybern. B, Cybern.*, vol. 28, no. 3, pp. 376–386, Jun. 1998.

[27] I. B. Turksen and Z. Zhong, "An approximate analogical reasoning approach based on similarity measures," *IEEE Trans. Syst., Man, Cybern.*, vol. 18, no. 6, pp. 1049–1056, Nov./Dec. 1988.

[28] C. Wagner, S. Miller, J. M. Garibaldi, D. T. Anderson, and T. C. Havens, "From interval-valued data to general type-2 fuzzy sets," *IEEE Trans. Fuzzy Syst.*, vol. 23, no. 2, pp. 248–269, Apr. 2015.

[29] C. Wagner, A. Pourabdollah, J. McCulloch, R. John, and J. M. Garibaldi, "A similarity-based inference engine for non-singleton fuzzy logic systems," in *Proc. IEEE Int. Conf. Fuzzy Syst.*, Vancouver, BC, Canada, Jul. 2016, pp. 316–323.

[30] C. Wagner and H. Hagras, "Toward general type-2 fuzzy logic systems based on zSlices," *IEEE Trans. Fuzzy Syst.*, vol. 18, no. 4, pp. 637–660, Aug. 2010.

[31] D. Wu and J. M. Mendel, "Uncertainty measures for interval type-2 fuzzy sets," *Inf. Sci.*, vol. 177, no. 23, pp. 5378–5393, 2007.

[32] D. Wu and J. M. Mendel, "A vector similarity measure for linguistic approximation: Interval type-2 and type-1 fuzzy sets," *Inf. Sci.*, vol. 178, no. 2, pp. 381–402, 2008.

[33] D. Wu and J. M. Mendel, "A comparative study of ranking methods, similarity measures and uncertainty measures for interval type-2 fuzzy sets," *Inf. Sci.*, vol. 179, no. 8, pp. 1169–1192, 2009.

[34] D. Wu and J. M. Mendel, "Perceptual reasoning for perceptual computing: A similarity-based approach," *IEEE Trans. Fuzzy Syst.*, vol. 17, no. 6, pp. 1397–1411, Dec. 2009.

[35] D. Wu, J. M. Mendel, and S. Coupland, "Enhanced Interval Approach for encoding words into interval type-2 fuzzy sets and its convergence analysis," *IEEE Trans. Fuzzy Syst.*, vol. 20, no. 3, pp. 499–513, Jun. 2012.

[36] D. Wu and W. W. Tan, "Genetic learning and performance evaluation of type-2 fuzzy logic controllers," *Eng. Appl. Artif. Intell.*, vol. 19, no. 8, pp. 829–841, 2006.

[37] D. Wu and W. W. Tan, "A simplified type-2 fuzzy controller for real-time control," *ISA Trans.*, vol. 15, no. 4, pp. 503–516, 2006.
[38] M.-S. Yang and D.-C. Lin, "On similarity and inclusion measures between type-2 fuzzy sets with an application to clustering," *Comput. Math. Appl.*, vol. 57, pp. 896–907, 2009.
[39] L. A. Zadeh, "Fuzzy sets," *Inf. Control*, vol. 8, pp. 338–353, 1965.
[40] L. A. Zadeh, "The concept of a linguistic variable and its application to approximate reasoning-1," *Inf. Sci.*, vol. 8, pp. 199–249, 1975.
[41] D. Zhai and J. M. Mendel, "Uncertainty measures for general type-2 fuzzy sets," *Inf. Sci.*, vol. 181, pp. 503–518, 2011.
[42] T. Zhao, J. Xiao, Y. Li, and X. Deng, "A new approach to similarity and inclusion measures between general type-2 fuzzy sets," *Soft Comput.*, vol. 18, no. 4, pp. 809–823, 2014.

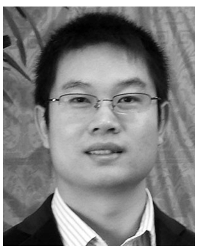

Dongrui Wu (S'05–M'09–SM'14) received the Ph.D. degree in electrical engineering from the University of Southern California, Los Angeles, CA, USA, in 2009.

He was a Lead Researcher with GE Global Research and the Chief Scientist of several startups. He is currently a Professor with the School of Automation, Huazhong University of Science and Technology, Wuhan, China. He has authored or coauthored more than 100 publications, including a book entitled *Perceptual Computing* (New York, NY, USA: Wiley–IEEE Press, 2010). His research interests include affective computing, brain–computer interface, computational intelligence, and machine learning.

Prof. Wu was a recipient of the IEEE Computational Intelligence Society Outstanding Ph.D. Dissertation Award in 2012, the IEEE TRANSACTIONS ON FUZZY SYSTEMS Outstanding Paper Award in 2014, the NAFIPS Early Career Award in 2014, and the IEEE Systems, Man, and Cybernetics Society Early Career Award in 2017. He is an Associate Editor for the IEEE TRANSACTIONS ON FUZZY SYSTEMS, the IEEE TRANSACTIONS ON HUMAN–MACHINE SYSTEMS, and the IEEE COMPUTATIONAL INTELLIGENCE MAGAZINE.

Jerry M. Mendel (LF'04) received the Ph.D. degree in electrical engineering from the Polytechnic Institute of Brooklyn, Brooklyn, NY, USA, in 1963.

He is currently an Emeritus Professor of electrical engineering with the University of Southern California, Los Angeles, CA, USA, where he has been since 1974. He is also the Tianjin 1000-Talents Foreign Experts Plan Endowment Professor and Honorary Dean of the College of Artificial Intelligence, Tianjin Normal University, Tianjin, China. He has authored or coauthored more than 570 technical papers and 13 books, including *Uncertain Rule-Based Fuzzy Systems: Introduction and New Directions* (2nd ed. New York, NY, USA: Springer, 2017), *Perceptual Computing: Aiding People in Making Subjective Judgments* (New York, NY, USA: Wiley–IEEE Press, 2010), and *Introduction to Type-2 Fuzzy Logic Control: Theory and Application* (New York, NY, USA: Wiley–IEEE Press, 2014). His current research interests include type-2 fuzzy logic systems and computing with words.

Dr. Mendel is a distinguished member of the IEEE Control Systems Society and a Fellow of the International Fuzzy Systems Association. He was the President of the IEEE Control Systems Society in 1986, a member of the Administrative Committee of the IEEE Computational Intelligence Society for nine years, and the Chairman of its Fuzzy Systems Technical Committee (TC) and the Computing With Words Task Force of that TC. He was a recipient of the 1983 Best Transactions Paper Award of the IEEE Geoscience and Remote Sensing Society, the 1992 Signal Processing Society Paper Award, the 2002 and 2014 Transactions on Fuzzy Systems Outstanding Paper Awards, a 1984 IEEE Centennial Medal, an IEEE Third Millennium Medal, a Fuzzy Systems Pioneer Award (2008) from the IEEE Computational Intelligence Society for "fundamental theoretical contributions and seminal results in fuzzy systems," and the 2015 USC Viterbi School of Engineering Senior Research Award.